Wide Band Proton sensor using Diamond Detector

Neeraj Maan
Roll No: MS13069

A dissertation submitted for the partial fulfilment
of BS-MS dual degree in Science

Under the guidance of
Dr. Satyajit Jena

April 2018

Indian Institute of Science Education and Research Mohali
Sector - 81, SAS Nagar, Mohali 140306, Punjab, India

Certificate of Examination

This is to certify that the dissertation titled **"Wide Band Proton sensor using Diamond Detector "** submitted by **Neeraj Maan** (Reg. No. MS13069) for the partial fulfillment of the BS-MS dual degree programme of the Institute, has been examined by the thesis committee duly appointed by the Institute. The committee finds the work done by the candidate satisfactory and recommends that the report be accepted.

Dr. Ananth Venkatesan	Dr. K. P. Singh	Dr. Satyajit Jena
		(Supervisor)

Dated: 20.04.2018

Declaration

The work presented in this dissertation has been carried out by me under the guidance of Dr. Satyajit Jena at the Indian Institute of Science Education and Research Mohali.

This work has not been submitted in part or in full for a degree, a diploma, or a fellowship to any other university or institute. Whenever contributions of others are involved, every effort is made to indicate this clearly, with due acknowledgement of collaborative research and discussions. This thesis is a bonafide record of original work done by me and all sources listed within have been detailed in the bibliography.

Neeraj Maan
(Candidate)

Dated: April 20, 2018

In my capacity as the supervisor of the candidate's project work, I certify that the above statements by the candidate are true to the best of my knowledge.

Dr. Satyajit Jena
(Supervisor)

Acknowledgement

I would first like to thank my thesis supervisor Dr. Satyajit Jena, who guided me through all my work. His help, motivation and encouragement was the driving factors in completion of my thesis work.
I would also like to thank the senior's in our lab Rohit Gupta , Nishat Fiza and Kartik. Without their participation and input , the work could never have been successfully completed.
I would like to acknowledge my lab mates with whom I had this one year journey and made the lab feel like a second home. Akhil , Asish , Anjaly , Shahina , Shubham and Tasha .
At last I would like to thank my parents who always pushed me forward and were always the source of positive energy for me. Thank you for everything.

Neeraj Maan
MS13069
IISER Mohali.

Contents

List of Figures

Abstract

The aim of current high energy experiments is to better understand the fundamental structure of universe by studying the properties of fundamental particles as given by the standard model. With the recent discovery of Higgs boson in 2012 it has provided us with more confidence to go beyond the standard model and search for similar heavier particles as proposed by various theories which were unable to be confirmed because such particles belong in the TeV range.

For the same reason the experiments at LHC and other high energy labs are shifting to newer phase of particle accelerators. Currently most of the particle detector sensors are made of silicon and the change in the energy levels of the experiments have lead to a very harsh radiation environment for the detector systems.

The incident particles damage the silicon crystalline structure. Hence there is a need for new sensor material which can withstand such levels of radiations. Diamond serve as a excellent replacement for the current situation since it has a huge band gap, high carrier mobility and it is extremely dense.

Our goal will be to better understand how the diamond detector works and how we can improve its signal detection.

Chapter 1

Particle detectors

A particle detector or in more general terms radiation detector is a device used for the detection , tracking or identification of ionizing particles , those produced by nuclear decay, cosmic radiation or reactions in particle accelerators. Our main focus will be on learning how detectors work in the accelerators.

1.1 Basic principle of particle detection

The interaction of incoming particle with the detector material transfers energy to the material. There are various processes by which the deposition takes place. We will discuss in detail the mechanisms of energy deposition in the material. Since our main focus is on diamond detector we will be studying the solid-state detector in detail.
High energy particles interact with matter in different ways. Our goal will be to study interaction of those particles which are vital for the working of tracking detectors.
Different particles lose different amount of energy during the interaction process. In the solid state detectors the major process of energy loss is elastic scattering. The Bethe-Bloch equation describes the mean energy loss dE per unit length dx for charged particles (except electrons)

$$-<\frac{dE}{dx}>=Kz^2\frac{Z}{A}\frac{1}{\beta^2}[\frac{1}{2}\ln(\frac{2m_ec^2\beta^2\gamma^2W_m}{I^2})-\beta^2-\frac{\delta(\gamma\beta)}{2}$$

where
mass of particle is M,
speed is v,

and charge z,

$K = 4\pi N_A r_e m_e c^2$ is a constant,

Z is atomic number,

A is atomic mass of the absorber,

W_m is the maximum energy in a single collision,

I is the mean excitation energy

The relativistic quantities can be expressed by

$$gamma = \frac{1}{\sqrt{\beta}} = \frac{E}{Mc^2}$$

The above Bethe-Bloch formula is described for moderately relativistic particles in a region of $0.1 \leq \beta\gamma \leq 1000$ and for intermediate Z materials.

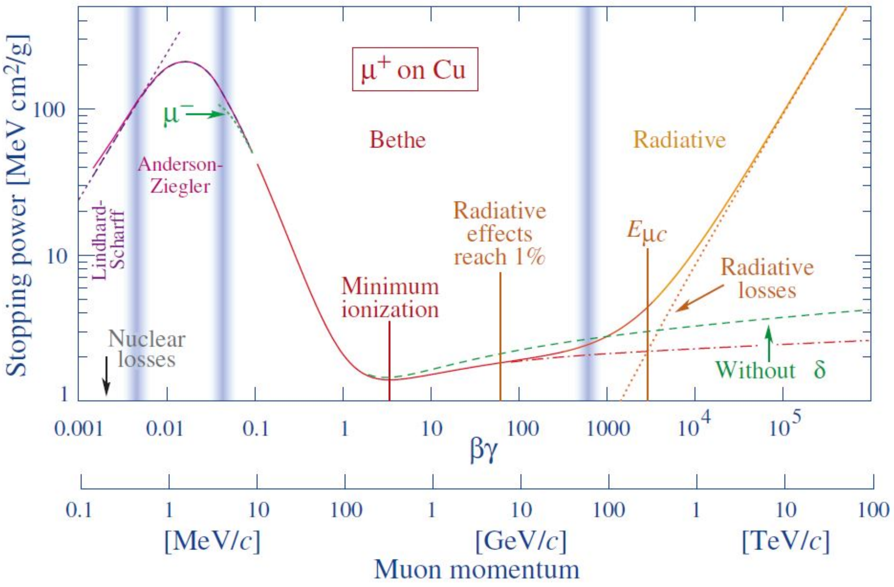

Figure 1.1: Bethe-Bloch diagram

Stopping power goes to minimum in the region of $\beta\gamma = 3 - 4$. Particles with mean energy loss rate through matter is close to this value are called Minimal Ionizing Particles(MIPs), the minimum energy loss for a MIP depends on detector material and roughly varies from $1MeV cm^2/g$ to $4MeV cm^2/g$. For experimental purposes the energy for particles can be considered to be close to energy loss of MIPs.

1.2 Interaction for Electron and positron

Electron and positron interaction requires modification in Bethe-Bloch formula. Since both particles have same mass the collision results in large energy transfer and large angle multiple scattering. The mean energy transfer $W_m = m_e c^2(\gamma - 1)/2$ is half of the energy transfer in the Bethe-Bloch equation because of the identical nature of scattering particles.

1.3 Photons

The photons interact with matter in a different way then that of charged particles. Following are the three effects that describe the interaction of photons.

1.3.1 Photoelectric effect

Photoelectric effect is the emission of electron or other free carriers when photon hits on a material. The radiation with atleast certain frequency known as threshold frequency will cause photoelectric effect. The photon is absorbed in this process and the electron emitted are termed as photoelectrons.

1.3.2 Compton scattering

It is the process when a photon scatters from an atomic electron, which recoils and carries off a fraction of the photon's energy.

1.3.3 Pair Production

When an high energy gamma ray ($E >> 2m_o c^2$) is incident then it leads to formation of positron-electron pair in the strong coulomb field of nucleus .

Depending on the energy of incident photon the contribution of the above three effects changes.

1.4 Neutrons

In comparison to other neutral hadrons, neutrons have a long time-life hence they can transverse particle detectors without decaying. Being neutral particles they don't participate in

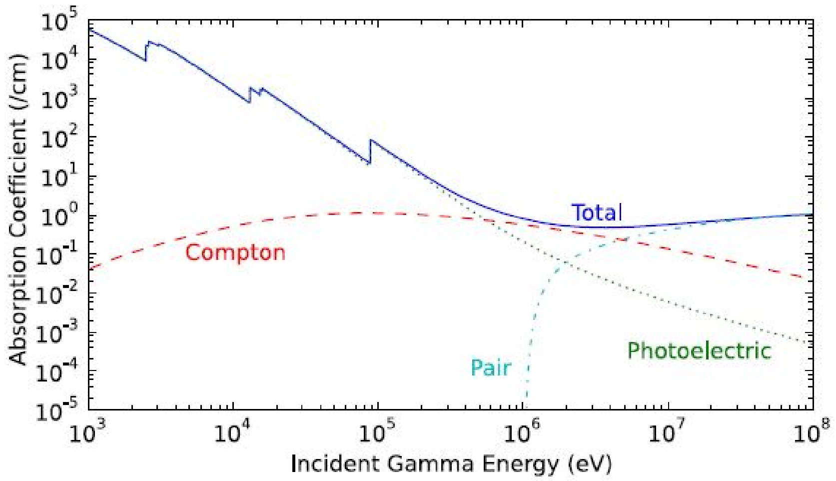

Figure 1.2: Total Energy absorption

electro-magnetic interaction with the electrons, however they interact with due to strong force with the nuclei. Since the strong force is a short ranged force hence probability of interaction is quite low.

1.5 Large Experimental setups

Large scale experiments such as the LHC experiments have layers of detectors around the collision space .These detectors measure properties of the long lived $(e^{\pm}, \mu^{p}m, \pi^{\pm}, k^{\pm}, p, \bar{p}, n)$ particles . The innermost detectors are usually precise tracking detector used to measure trajectories of short lived particles and hence able to identify and measure these particles. Since the recent discovery of Higgs Boson particle in 2012 it has provided us with much confidence to pursue experimentation in higher energy regime (COM energy of 13TeV-14TeV). This enable us to study and search for theorized heavy particles such as particles predicted by SUSY (SUperSYmetry). However, the increase in energy has lead to some problems in the detector system placed in places especially to the detectors placed nearest to the beam. The increase in energy has lead to higher radiation level environment hence damaging current generation of silicon made detectors.

1.6 New type of detector system

Being faced by the ineffectiveness of silicon detectors there is a need for a detector material to be used in place which can sustain high radiation damage and also have a good efficiency . Artificially manufactured diamond can serve as an excellent alternative since in comparison to silicon they have high rigidity and strength making them less vulnerable to radiation damage, higher band gap, higher resistivity and better resistance to corrosion. We will be discussing about the manufacture and working of these solid-state diamond detectors.

Chapter 2

Diamond detectors

2.1 Diamonds

Before going further into detector physics we should discuss properties of diamond. Diamond is an allotropic form of carbon with a highly stable structure due to sp^3 bonded carbon where each atom has four covalent bonds directed to vertices of of a regular tetrahedron. This leads to a cubic lattice of high strength and rigidity and bond length of 0.1545 nm.
And due to the strength and rigidity of its lattice diamond has great physical properties. It is the hardest substance on the planet. Other properties such as good thermal conductor at low and room temperature makes it a good choice for a detector material as due to hardness it is resistant against radiation damage and better carrier for charged particles because of conductivity. So we have established that diamond have high radiation and temperature tolerance for covalent bonds because of carbon's small atomic number.
While other semiconductor materials such as Si have a lower signal output with increasing temperature and irradiation. However diamond operates stably at high temperature and high radiation environment.

2.2 Chemical Vapor Deposition

The properties of diamond as discussed in the last chapter make it an excellent detector material but the question is which diamond to use for the experiments since the naturally occurring diamond is highly expensive and contains high level of impurities .
For the need for detectors , artificial diamond is manufactured by various methods, we will

discuss about the most commonly used ones of them all. For all the current detector grade diamond comes from synthesis of artificial diamond using various methods.

The most commonly used of of them are High-Pressure and High-temperature (HPHT)process and chemical vapor deposition(CVD). In HPHT we create high temperature and high pressure to produce diamonds.

In CVD we use a hydrocarbon gas mixture to grow diamond. This method involves a formation of thin layer of the material by deposition on a substrate from a gas phase consisting of hydrocarbon gases and hydrogen.This method is widely used because of its ability to grow larger diamonds(area-wise) and better check over impurities in diamond. CVD setup requires a rather low pressure (1 kPa -27 kPa). The process involves chemical reaction in a gas phase which happens over a solid surface . The gas is a mixture of methane and hydrogen.

There are two types of substrates that are used for the diamond growth process namely the homo-epitaxial and hetero-epitaxial substrates. For the homo-epitaxial substrate we use a diamond like material as a substrate. The homo-epitaxial growth method is used for the electronic grade diamonds.

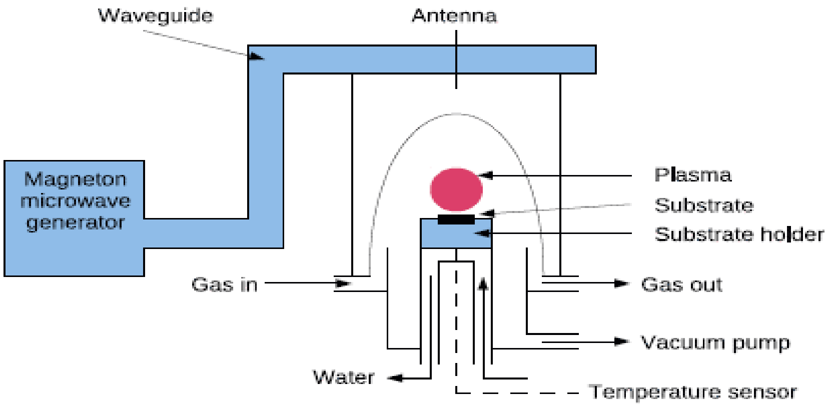

Figure 2.1: Chemical Vapor Depositon Appratus for scCVD

There are two types of diamonds grown from this process single crystalline CVD (scCVD) and poly-crystalline CVD (pCVD). The two types differ in the way they are grown, scCVD are grown on surface-treated High-pressure high-temperature diamonds. And in pCVD diamond the substrate consists of diamond powder. The use of diamond powder adds grain to the structure of pCVD diamonds.

2.3 Working of diamond detector

Diamond has a high carrier mobility hence enabling it to work as a solid-state ionization chamber.

A diamond detector has a thickness of around 350μm to 500μm. The electrodes for the detector are made up of high grade Chromium. Diamond has a high breakdown voltage hence it is possible to apply high bias voltage across the detector (1.5-2V/μm). So when the charged particles traverse through the material, atoms in the crystal lattice are ionized creating electron hole pairs where electrons move to the conduction band leaving holes in the valence band. The average amount of energy required to produce an electron-hole pair is 13.5eV.

Using the already discussed Bethe-Bloch equation we can calculate the average number of electrons and holes generated by one MIP in the 1μm thickness of diamond detector, we call this term as q_0 and its value comes out to be 36e/μm. These charge carriers travel across the material and are responsible for the signal. But we need a measure to quantify the signal created by this charge propagation, charge collection distance (CCD) is the amount of charge measured by the electronic system per value of q_0.

Chapter 3

Major experiments

3.1 Diamond neutron detectors for the JET Tokamak

The experiment was started with the setup of SCD detector covered with 2μm LiF film . The experiment aimed for the measurement of time dependent neutron emission from plasmas. The use of artificial diamond detectors for the use in nuclear detectors was started with the purpose to study physical properties of CVD films.

The first successful test for pCVD as 14MeV neutron detector in Tokamak was in 2003 in JET-TTE and considered to be a huge stepping stone for further experiments to come.One more advancement occurred with the introduction of boron doped conduction layer being grown on the substrate . It was fairly easy to reproduce this type of detector material and as before diamond detectors had low grade HPHT sCVD substrate which was not suitable as a detection material and had to be removed but adding of boron layer took away requirement to remove that layer. The substrate removal process was tough and expensive.Such improvements in the diamond detector performance helped in the working of harsh tokamak radiation environment.

3.1.1 Detector setup

The installation of LiDia detector took place in 2006. The detector was established with the lowest threshold to cover all the signals produced by neutrons regardless of their energy and with a second threshold for signals produced by only the 14MeV neutron. The detector system was set with a bias of $+3V/\mu m$ for the whole time till the end of JET experimental campaign, which ended in 2007.

3.1.2 Results from the detector

The experimental campaign at JET operated with the DD plasmas hence, the 14MeV emission was because of triton burn-up accounting for only around 1 percentage of total neutron emission. The cross section for reaction was also small and so is the detector volume. The above mentioned factors combined resulted in the poor counting statistics for the 14MeV neutrons with the detector system placed.

However, the positive aspects we found about the LiDia detector is the ability to detect neutrons at all energy levels as well as at 14MeV. This thing was confirmed when the emission pulse from LiDia and a silicon detector were compared and results pointed out the clear interpretation that although low in count but the detector was able to produce time dependent 14MeV neutron emission.

3.1.3 Conclusion

The results obtained from the SCD detectors at JET strongly suggest that diamond detectors are the right kind of detectors to be used at Tokamak.

Although the yield of experiment is not very great but can be improved by working on the detector manufacturing processes. The size of detector is also an issue, however it can be overcome by the use of specifically produced bigger sized diamond detectors or by using matrix of detectors.

The detector system was stable and reliable for the whole duration of experiment. The experiment encourages people around the world to develop better grade diamond detectors. For sure they are the future of detector physics.

3.2 scCVD Detector usage in space for plasma measurement

Since the artificial diamonds produced by CVD are more pure and bigger than natural diamond detectors hence, could be suitable for the measurement of space plasmas but falls short in use due to charge trap between the crystal boarders of the detector.

But with the current advancement in the SCD manufacturing techniques, the detectors produced now does not face the issue of charge trap anymore and hence could serve as the detector for space plasma energy measurements.

3.2.1 Detector

We use scCVD diamond by metallizing the surface with Al and Ti to create a metal-insulator-metal form of solid-state particle detector. For detector setup we use electron beam evaporation method along with Ion Bombardment Assisted Deposition and for surface metallisation we use 2keV Argon ions. For calibration source we use 250keV proton and He ion beams. And for calibration of detector response to electrons and alpha particles we use radioactive source.

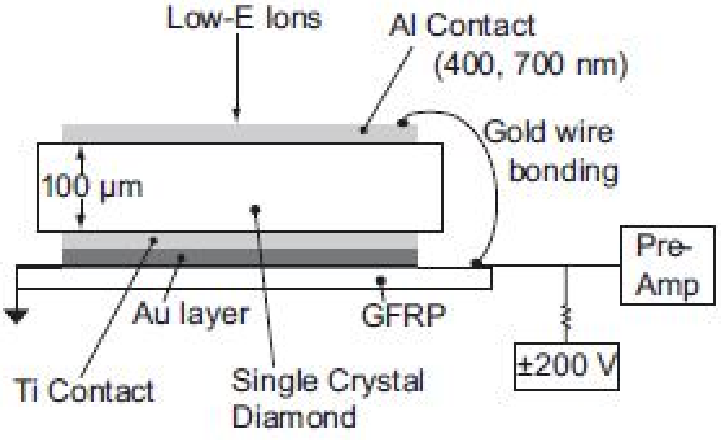

Figure 3.1: Diamond Detector fabricated for space usage

3.2.2 Result and inferance

The experiment was performed with two type of diamond detectors with different Al lengths. The two different types of detectors helped us in characterizing the energy loss and measuring the intrinsic noise performance of the detector.

Because of strong cohesive energy diamond forms denser crystal structure than silicon hence, we observe higher radiation hardness and stopping power for diamond. Also diamond have huge band gap meaning very low free charge carrier concentration resulting in minimal shot noise.

Another advantage of diamond detector is fast electron and hole mobility enabling in fast time analysis (of the order < 1 ns).

3.2.3 Conclusion

There is a successful attempt to manufacture artificial diamond detector for measurement of plasma and energetic particles in space. The observed results for energy range and threshold levels for diamond are as per as silicon detectors but the ability to handle harsh radiation environment makes diamond a better candidate for the detector system.

3.3 HT characterization of charge collection efficiency

As already discussed diamond has high temperature and radiation tolerance hence it is ideal for the high temperature and high radiation environment of gamma-ray detectors of containment atmospheric monitoring system (CAMS). Also unlike Si, diamond has unchanged semiconductor properties under influence of neutrons.

For the detector part, sCVD detector grade diamond was used. The diamond was grown with microwave plasma CVD process, with the dimensions $72 \times 5 \times 5 mm^2$. For fabrication, metal electrodes were used on both sides of the diamond.

3.3.1 Results

The I-V characteristic graph was measured in order to evaluate leakage current. Next step included measurement of induced charge distribution by alpha particles using both positive and negative bias.

The CCE of holes obtained was 96.9 percentage and energy resolution of 3 percentage at 474 K but no CCE was obtained for electrons above 373 K. The experiment suffered from incident direction and surface leakage current. The leakage current seems to increase at high temperature because of rise in vacancy and interstitial centers .

The use of high-purity diamond and guard ring for the connector can be used to minimize the leakage current.

3.4 Diamond detectors for fast neutron monitoring

The properties of diamond such as higher bandgap, higher resistivity and e-h mobility make it very suitable for radiation detector applications. With the advancement in artificial diamond fabrication, diamond is now used for majority of ionizing radiation detection such as alpha, gamma, UV rays, electrons, protons and neutrons.

Because of the ability of diamond detector to operate at high temperature make them a good option for monitoring fast neutrons produced by the D-T nuclear fusion reactions in advanced fusion facilities.

scCVD diamond detectors have 100 percentage charge collection and provide around 1 percentage energy resolution for neutrons and charged particles and pCVD diamond structure has high defect concentration and it causes trapping and charge recombination resulting in charge built up and polarization effects.

With the improvement in CVD now it is possible to fabricate detector grade substrate. This is further used for characterization and measurement .

3.4.1 Results

The I-V characteristics was obtained for the fabricated detectors. The electric field was maintained at $1V/\mu$m. Observed leakage current was very low, 4nA at 100V bias for 100μm. The leakage current for pCVD and scCVD seems to vary from pA to nA depending on the detector dimensions and way of fabrication.

The detector was operated for several hours straight inorder to check its stability . The alpha response was unstable with time. This was the result of charge trapping in the detector .

Hence, the count rates went down with time. When the same measurement of alpha source was repeated with β-irradiation. With this change there was increase in count rates probably because of filling of traps. Also now the alpha response was stable with time.

3.4.2 Conclusion

Artificial diamond was fabricated with pCVD substrate. The detector worked fine but was unstable with time. The instability was fixed with the help of irradiation of the detector with β-source.

Experiment data with different dimension of diamond showed that $100\mu m$ diamond detector is more suited for neutron measurement than $300\mu m$ even though interaction probability of neutron with carbon is better in thicker diamond detector. The experiment was successful for neutron measurement at room temperature with the use of a D-T fast neutron detector in the range $2.86 \times 10^5 n/stimescm^2$ to $8.76times10^6 n/stimescm^2$.

However, the pCVD diamond detectors provides information about neutron rates, there is a need for diamond detector which can provide us with energy information, as well.

Chapter 4

Simulations and Results

4.1 Weightfield 2 simulations

Weightfield 2 is a simulation tool used for the study of signals in ultra fast silicon and diamond detectors. It is written in the C$++$ language and its interface is developed from the ROOT interface TGUI.

4.1.1 Working

The program in the tool calculates the amount of induced current with the help of Ramo's Theorem.
The theorem follows as:

$$I = -\frac{q.E_A.v}{V_A}$$

where,
I is current delivered to voltage source as charge e moves,
E_A is the electric field at the position of charge q,
V_A is the potential of the conductor A,
v is the instantaneous velocity of the charge q,
So lets suppose there are charges $+q$ and $-q$ moving a distance x in the electric field E then the work done to maintain the electric field is qxE. If the width of the detector is L and

potential difference is V then

$$W = \frac{qxV}{L}, Q = \frac{qx}{l}$$

Therefore, the charge that flows to the electrode A while electron move a distance d is q_A.

$$q_A = \frac{qd}{L}$$

After calculating current , it draws electric field and allows user to set temperature, magnetic field, gain and other various factors. It also consists the option of simulating oscilloscope.

4.1.2 Graphical interface

Here are some of the basic simulations from the Weightfield 2 simulator is carried out inorder to get a better insight of the tool.

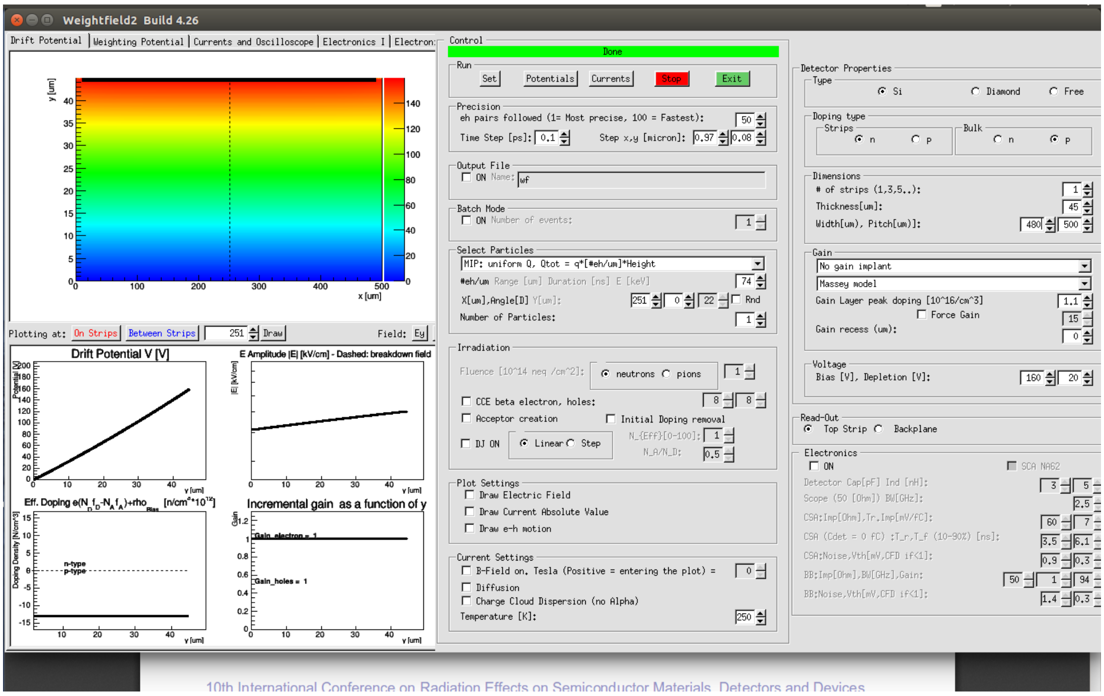

Weightfield2 Build 4.26

Control: Done

Run: Set | Potentials | Currents | Stop | Exit

Precision
eh pairs followed (1= Most precise, 100 = Fastest): 50
Time Step [ps]: 0.1   Step x,y [micron]: 0.97 0.08

Output File
☐ ON Name: wf

Batch Mode
☐ ON Number of events: 1

Select Particles
MIP: uniform Q, Qtot = q*[#eh/um]*Height
#eh/um Range [um] Duration [ns] E [keV]: 74
X[um],Angle[D] Y[um]: 251 0 22 ☐ Rnd
Number of Particles: 1

Irradiation
Fluence [10^14 neq /cm^2]: ● neutrons ○ pions 1
☐ CCE beta electron, holes: 8 8
☐ Acceptor creation   ☐ Initial Doping removal
☐ DJ ON ● Linear ○ Step   N_{Eff}[0-100]: 1   N_A/N_D: 0.5

Plot Settings
☐ Draw Electric Field
☐ Draw Current Absolute Value
☐ Draw e-h motion

Current Settings
☐ B-Field on, Tesla (Positive = entering the plot) = 0
☐ Diffusion
☐ Charge Cloud Dispersion (no Alpha)
Temperature [K]: 250

Detector Properties
Type: ● Si ○ Diamond ○ Free
Doping type: Strips ● n ○ p   Bulk ○ n ● p
Dimensions
# of strips (1,3,5,.): 1
Thickness[um]: 45
Width[um), Pitch[um)]: 480 500
Gain
No gain implant
Massey model
Gain Layer peak doping [10^16/cm^3]: 1.1
☐ Force Gain: 15
Gain recess (um): 0
Voltage
Bias [V], Depletion [V]: 160 20

Read-Out: ● Top Strip ○ Backplane

Electronics
☐ ON   ☐ SCA NA62
Detector Cap[pF] Ind [nH]: 3 5
Scope (50 [Ohm]) BW[GHz]: 2.5
CSA:Imp[Ohm],Tr.Imp[mV/fC]: 60 7
CSA (Cdet = 0 fC) :T_r,T_f (10-90%) [ns]: 3.5 6.1
CSA:Noise,Vth[mV,CFD if<1]: 0.9 0.3
BB:Imp[Ohm],BW[GHz],Gain: 50 1 94
BB:Noise,Vth[mV,CFD if<1]: 1.4 0.3

Plotting at: On Strips | Between Strips | 251 | Draw   Field: Ey

Figure 4.1: Drift potential, no of stripes-1

From the simulation results we can see that it works well for signal detection with low gain. After this we carried out some more advanced simulations varying various factors.

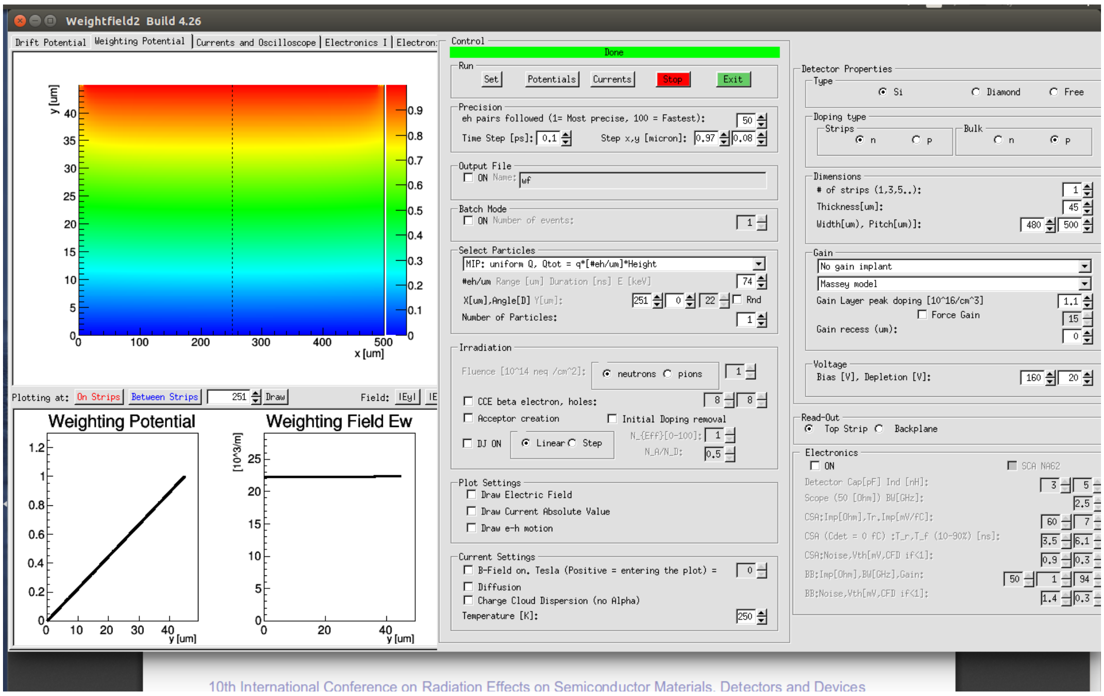

Plotting at: 251

Precision
eh pairs followed (1= Most precise, 100 = Fastest): 50
Time Step [ps]: 0.1
Step x,y [micron]: 0.97 0.08

Output File
☐ ON Name: wf

Batch Mode
☐ ON Number of events: 1

Select Particles
MIP: uniform Q, Qtot = q*[#eh/um]*Height
#eh/um Range [um] Duration [ns] E [keV] 74
X[um],Angle[D] Y[um]: 251 0 22 ☐ Rnd
Number of Particles: 1

Irradiation
Fluence [10^14 neq /cm^2]: ● neutrons ○ pions 1
☐ CCE beta electron, holes: 8 8
☐ Acceptor creation
☐ Initial Doping removal
☐ DJ ON ● Linear ○ Step
N_{Eff}[0-100]: 1
N_A/N_D: 0.5

Plot Settings
☐ Draw Electric Field
☐ Draw Current Absolute Value
☐ Draw e-h motion

Current Settings
☐ B-Field on, Tesla (Positive = entering the plot) = 0
☐ Diffusion
☐ Charge Cloud Dispersion (no Alpha)
Temperature [K]: 250

Detector Properties
Type
● Si ○ Diamond ○ Free
Doping type
Strips ● n ○ p
Bulk ○ n ● p
Dimensions
# of strips (1,3,5..): 1
Thickness[um]: 45
Width[um), Pitch[um)]: 480 500
Gain
No gain implant
Massey model
Gain Layer peak doping [10^16/cm^3] 1.1
☐ Force Gain 15
Gain recess (um): 0
Voltage
Bias [V], Depletion [V]: 160 20

Read-Out
● Top Strip ○ Backplane

Electronics
☐ ON
☐ SCA NA62
Detector Cap[pF] Ind [nH]: 3 5
Scope (50 [Ohm]) BW[GHz]: 2.5
CSA:Imp[Ohm],Tr.Imp[mV/fC]: 60 7
CSA (Cdet = 0 fC) :T_r,T_f (10-90%) [ns]: 3.5 6.1
CSA:Noise,Vth[mV,CFD if<1]: 0.9 0.3
BB:Imp[Ohm],BW[GHz],Gain: 50 1 94
BB:Noise,Vth[mV,CFD if<1]: 1.4 0.3

Figure 4.2: Weighting potential, no of stripes-1

4.2 Leakage Current

Leakage current in diamond is due to limited electric conductivity inherent in the semiconductor material. It is of two types bulk and surface leakage current.

Bulk leakage current is due to the those carriers that are thermally energetic to cross the diamond band gap and it is inversely proportional to carrier lifetime. The surface leakage current is attributed to the manufacturing, process, measurement methods, electrode conductivity .

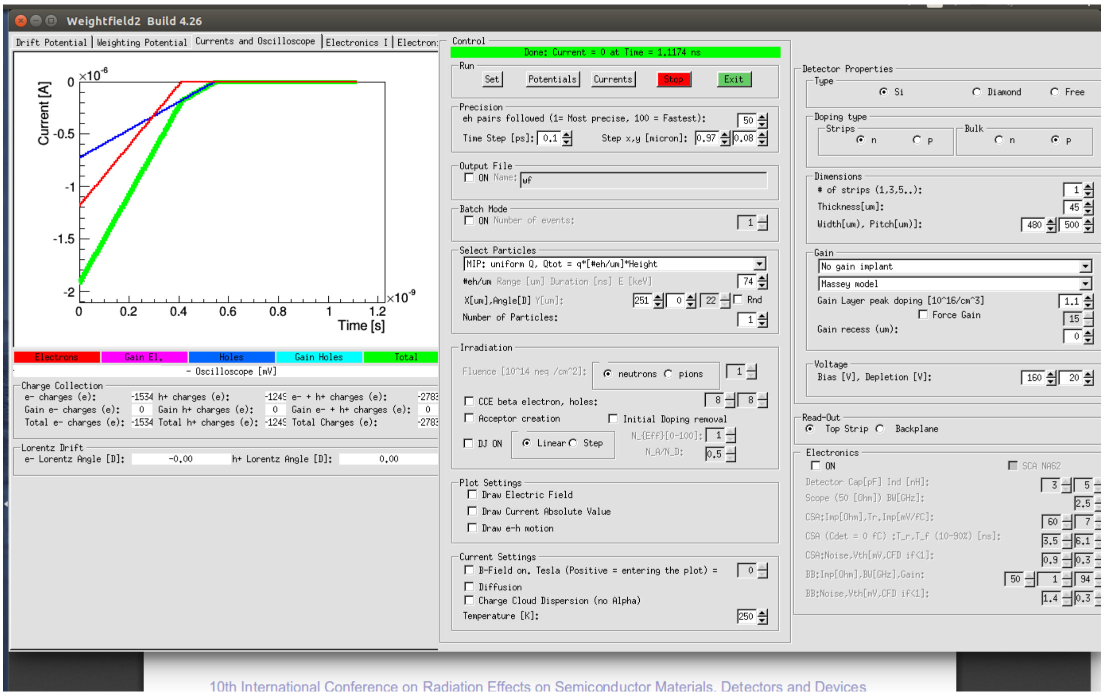

Charge Collection
e- charges (e): -1534 h+ charges (e): -1249 e- + h+ charges (e): -2783
Gain e- charges (e): 0 Gain h+ charges (e): 0 Gain e- + h+ charges (e): 0
Total e- charges (e): -1534 Total h+ charges (e): -1249 Total Charges (e): -2783

Lorentz Drift
e- Lorentz Angle [D]: -0.00 h+ Lorentz Angle [D]: 0.00

Control
Done: Current = 0 at Time = 1.1174 ns

Precision
eh pairs followed (1= Most precise, 100 = Fastest): 50
Time Step [ps]: 0.1 Step x,y [micron]: 0.97 0.08

Output File
☐ ON Name: wf

Batch Mode
☐ ON Number of events: 1

Select Particles
MIP: uniform Q, Qtot = q*[#eh/um]*Height
#eh/um Range [um] Duration [ns] E [keV]: 74
X[um],Angle[D] Y[um]: 251 0 22 ☐ Rnd
Number of Particles: 1

Irradiation
Fluence [10^14 neq /cm^2]: ● neutrons ○ pions 1
☐ CCE beta electron, holes: 8 8
☐ Acceptor creation ☐ Initial Doping removal
☐ DJ ON ● Linear ○ Step N_{Eff}[0-100]: 1
N_A/N_D: 0.5

Plot Settings
☐ Draw Electric Field
☐ Draw Current Absolute Value
☐ Draw e-h motion

Current Settings
☐ B-Field on. Tesla (Positive = entering the plot) = 0
☐ Diffusion
☐ Charge Cloud Dispersion (no Alpha)
Temperature [K]: 250

Detector Properties
Type: ● Si ○ Diamond ○ Free
Doping type: Strips ● n ○ p; Bulk ○ n ● p

Dimensions
# of strips (1,3,5..): 1
Thickness[um]: 45
Width[um), Pitch[um)]: 480 500

Gain
No gain implant
Massey model
Gain Layer peak doping [10^16/cm^3] 1.1
☐ Force Gain 15
Gain recess (um): 0

Voltage
Bias [V], Depletion [V]: 160 20

Read-Out
● Top Strip ○ Backplane

Electronics
☐ ON ☐ SCA NA62
Detector Cap[pF] Ind [nH]: 3 5
Scope (50 [Ohm]) BW[GHz]: 2.5
CSA:Imp[Ohm],Tr.Imp[mV/fC]: 60 7
CSA (Cdet = 0 fC) :T_r,T_f (10-90%) [ns]: 3.5 6.1
CSA:Noise,Vth[mV,CFD if<1]: 0.9 0.3
BB:Imp[Ohm],BW[GHz],Gain: 50 1 94
BB:Noise,Vth[mV,CFD if<1]: 1.4 0.3

Figure 4.3: Currents, no of stripes-1

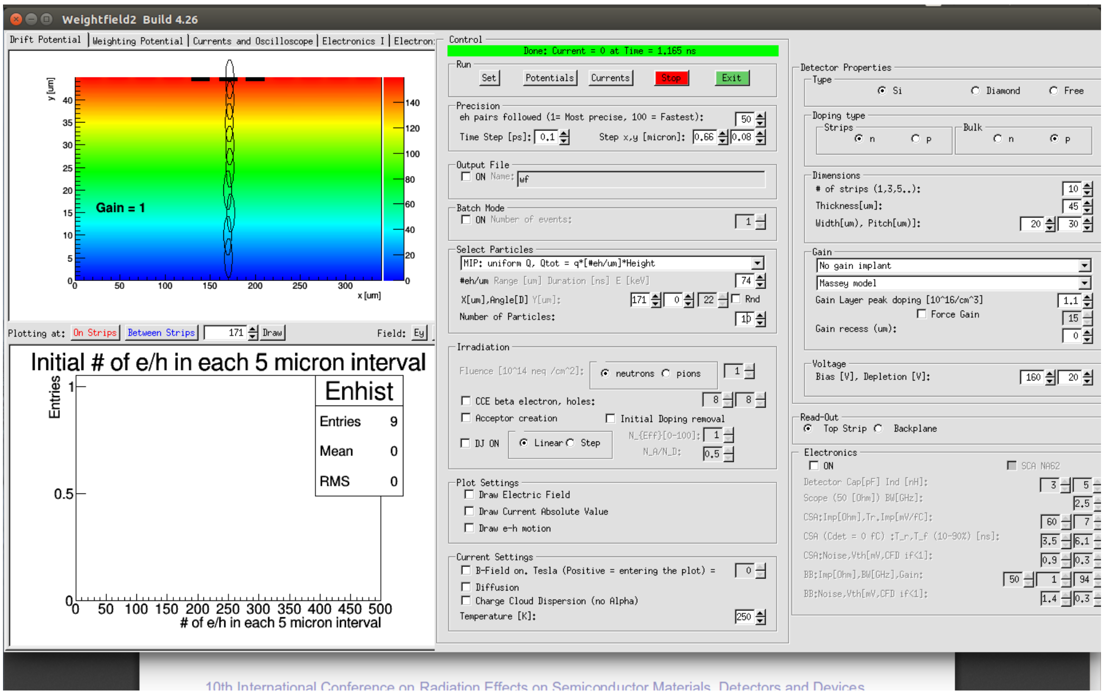

Plotting at: 171

Enhist	
Entries	9
Mean	0
RMS	0

Control
Done: Current = 0 at Time = 1.165 ns

Precision
eh pairs followed (1= Most precise, 100 = Fastest): 50
Time Step [ps]: 0.1 Step x,y [micron]: 0.66 0.08

Output File
☐ ON Name: wf

Batch Mode
☐ ON Number of events: 1

Select Particles
MIP: uniform Q, Qtot = q*[#eh/um]*Height
#eh/um Range [um] Duration [ns] E [keV]: 74
X[um],Angle[D] Y[um]: 171 0 22 ☐ Rnd
Number of Particles: 10

Irradiation
Fluence [10^14 neq /cm^2]: ● neutrons ○ pions 1
☐ CCE beta electron, holes: 8 8
☐ Acceptor creation ☐ Initial Doping removal
☐ DJ ON ● Linear ○ Step N_{Eff}[0-100]: 1
N_A/N_D: 0.5

Plot Settings
☐ Draw Electric Field
☐ Draw Current Absolute Value
☐ Draw e-h motion

Current Settings
☐ B-Field on. Tesla (Positive = entering the plot) = 0
☐ Diffusion
☐ Charge Cloud Dispersion (no Alpha)
Temperature [K]: 250

Detector Properties
Type: ● Si ○ Diamond ○ Free
Doping type: Strips ● n ○ p; Bulk ○ n ● p

Dimensions
# of strips (1,3,5..): 10
Thickness[um]: 45
Width[um), Pitch[um)]: 20 30

Gain
No gain implant
Massey model
Gain Layer peak doping [10^16/cm^3] 1.1
☐ Force Gain 15
Gain recess (um): 0

Voltage
Bias [V], Depletion [V]: 160 20

Read-Out
● Top Strip ○ Backplane

Electronics
☐ ON ☐ SCA NA62
Detector Cap[pF] Ind [nH]: 3 5
Scope (50 [Ohm]) BW[GHz]: 2.5
CSA:Imp[Ohm],Tr.Imp[mV/fC]: 60 7
CSA (Cdet = 0 fC) :T_r,T_f (10-90%) [ns]: 3.5 6.1
CSA:Noise,Vth[mV,CFD if<1]: 0.9 0.3
BB:Imp[Ohm],BW[GHz],Gain: 50 1 94
BB:Noise,Vth[mV,CFD if<1]: 1.4 0.3

Figure 4.4: Drift potential, no of stripes-10

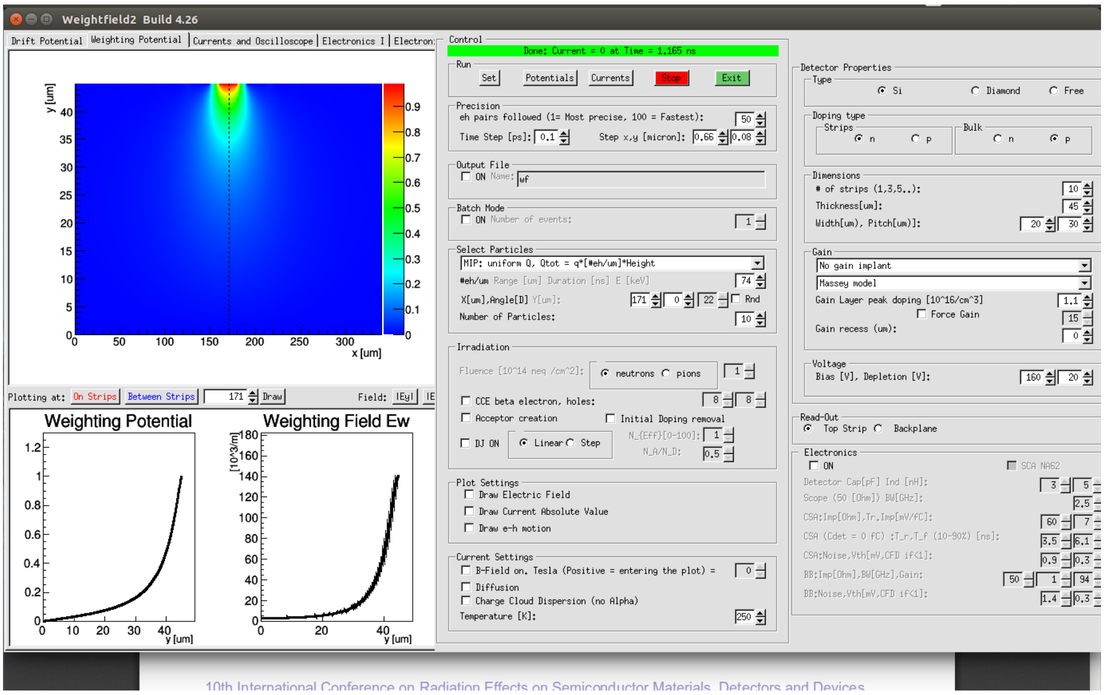

Plotting at: On Strips Between Strips 171

Field: |Ey|

Done: Current = 0 at Time = 1.165 ns

Precision
eh pairs followed (1= Most precise, 100 = Fastest): 50
Time Step [ps]: 0.1 Step x,y [micron]: 0.66 0.08

Output File
☐ ON Name: wf

Batch Mode
☐ ON Number of events: 1

Select Particles
MIP: uniform Q, Qtot = q*[#eh/um]*Height
#eh/um Range [um] Duration [ns] E [keV] 74
X[um],Angle[D] Y[um]: 171 0 22 ☐ Rnd
Number of Particles: 10

Irradiation
Fluence [10^14 neq /cm^2]: ● neutrons ○ pions 1
☐ CCE beta electron, holes: 8 8
☐ Acceptor creation ☐ Initial Doping removal
☐ DJ ON ● Linear ○ Step N_{Eff}[0-100]: 1
N_A/N_D: 0.5

Plot Settings
☐ Draw Electric Field
☐ Draw Current Absolute Value
☐ Draw e-h motion

Current Settings
☐ B-Field on, Tesla (Positive = entering the plot) = 0
☐ Diffusion
☐ Charge Cloud Dispersion (no Alpha)
Temperature [K]: 250

Detector Properties
Type
● Si ○ Diamond ○ Free
Doping type
Strips ● n ○ p
Bulk ○ n ● p
Dimensions
# of strips (1,3,5..): 10
Thickness[um]: 45
Width[um), Pitch[um)]: 20 30
Gain
No gain implant
Massey model
Gain Layer peak doping [10^16/cm^3] 1.1
☐ Force Gain 15
Gain recess (um): 0
Voltage
Bias [V], Depletion [V]: 160 20

Read-Out
● Top Strip ○ Backplane

Electronics
☐ ON ☐ SCA NA62
Detector Cap[pF] Ind [nH]: 3 5
Scope (50 [Ohm]) BW[GHz]: 2.5
CSA:Imp[Ohm],Tr.Imp[mV/fC]: 60 7
CSA (Cdet = 0 fC) :T_r,T_f (10-90%) [ns]: 3.5 6.1
CSA:Noise,Vth[mV,CFD if<1]: 0.9 0.3
BB:Imp[Ohm],BW[GHz],Gain: 50 1 94
BB:Noise,Vth[mV,CFD if<1]: 1.4 0.3

Figure 4.5: Weighting potential, no of stripes-10

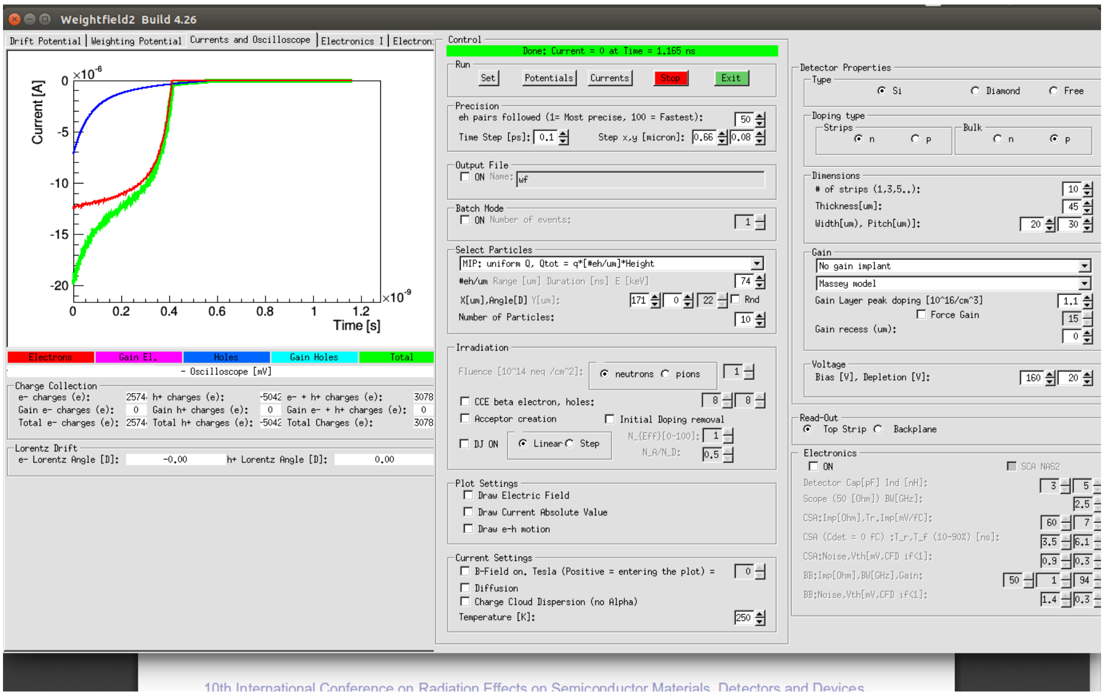

Charge Collection
e- charges (e): 2574 h+ charges (e): -5042 e- + h+ charges (e): 3078
Gain e- charges (e): 0 Gain h+ charges (e): 0 Gain e- + h+ charges (e): 0
Total e- charges (e): 2574 Total h+ charges (e): -5042 Total Charges (e): 3078

Lorentz Drift
e- Lorentz Angle [D]: -0.00 h+ Lorentz Angle [D]: 0.00

Done: Current = 0 at Time = 1.165 ns

Precision
eh pairs followed (1= Most precise, 100 = Fastest): 50
Time Step [ps]: 0.1 Step x,y [micron]: 0.66 0.08

Output File
☐ ON Name: wf

Batch Mode
☐ ON Number of events: 1

Select Particles
MIP: uniform Q, Qtot = q*[#eh/um]*Height
#eh/um Range [um] Duration [ns] E [keV] 74
X[um],Angle[D] Y[um]: 171 0 22 ☐ Rnd
Number of Particles: 10

Irradiation
Fluence [10^14 neq /cm^2]: ● neutrons ○ pions 1
☐ CCE beta electron, holes: 8 8
☐ Acceptor creation ☐ Initial Doping removal
☐ DJ ON ● Linear ○ Step N_{Eff}[0-100]: 1
N_A/N_D: 0.5

Plot Settings
☐ Draw Electric Field
☐ Draw Current Absolute Value
☐ Draw e-h motion

Current Settings
☐ B-Field on, Tesla (Positive = entering the plot) = 0
☐ Diffusion
☐ Charge Cloud Dispersion (no Alpha)
Temperature [K]: 250

Detector Properties
Type
● Si ○ Diamond ○ Free
Doping type
Strips ● n ○ p
Bulk ○ n ● p
Dimensions
# of strips (1,3,5..): 10
Thickness[um]: 45
Width[um), Pitch[um)]: 20 30
Gain
No gain implant
Massey model
Gain Layer peak doping [10^16/cm^3] 1.1
☐ Force Gain 15
Gain recess (um): 0
Voltage
Bias [V], Depletion [V]: 160 20

Read-Out
● Top Strip ○ Backplane

Electronics
☐ ON ☐ SCA NA62
Detector Cap[pF] Ind [nH]: 3 5
Scope (50 [Ohm]) BW[GHz]: 2.5
CSA:Imp[Ohm],Tr.Imp[mV/fC]: 60 7
CSA (Cdet = 0 fC) :T_r,T_f (10-90%) [ns]: 3.5 6.1
CSA:Noise,Vth[mV,CFD if<1]: 0.9 0.3
BB:Imp[Ohm],BW[GHz],Gain: 50 1 94
BB:Noise,Vth[mV,CFD if<1]: 1.4 0.3

Figure 4.6: Currents, no of stripes-10

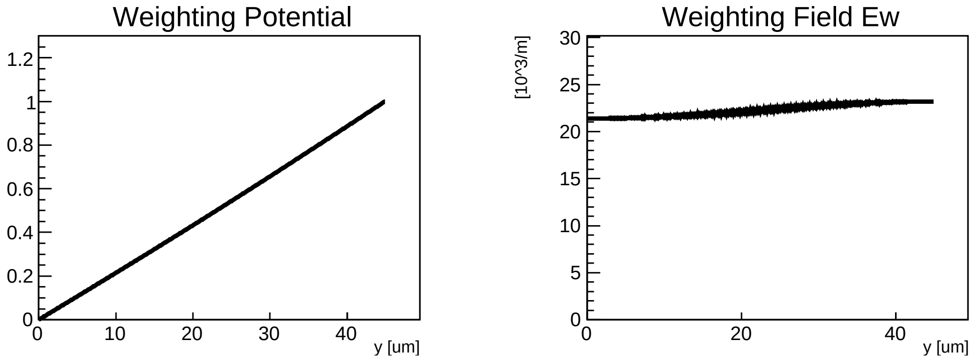

Figure 4.7: Weighting field and potential, Width=45μ m, stripes=1

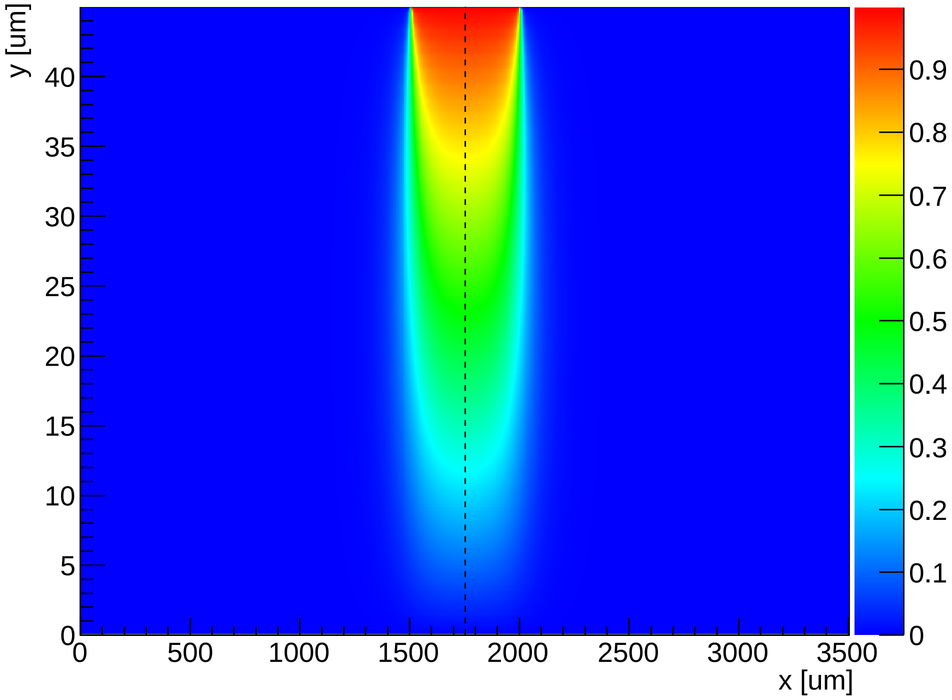

Figure 4.8: Weighting field and potential, Width=45μ m, stripes=1

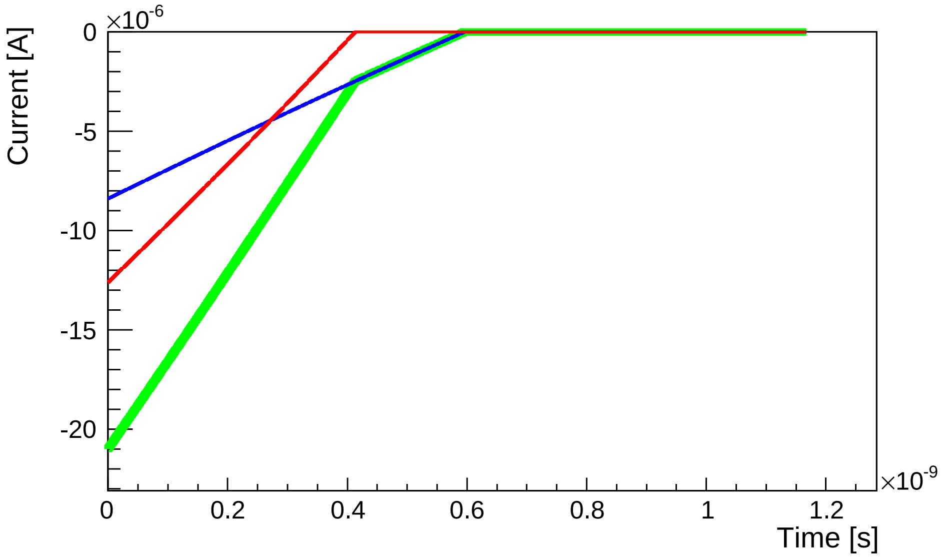

Figure 4.9: Currents, Width=45μ m, stripes=1

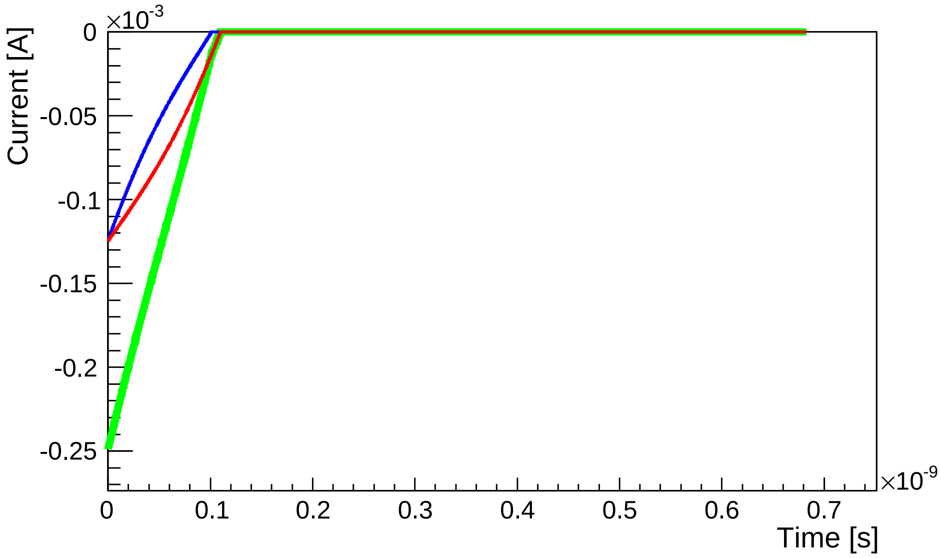

Figure 4.10: Currents, Width=25μ m, stripes=1

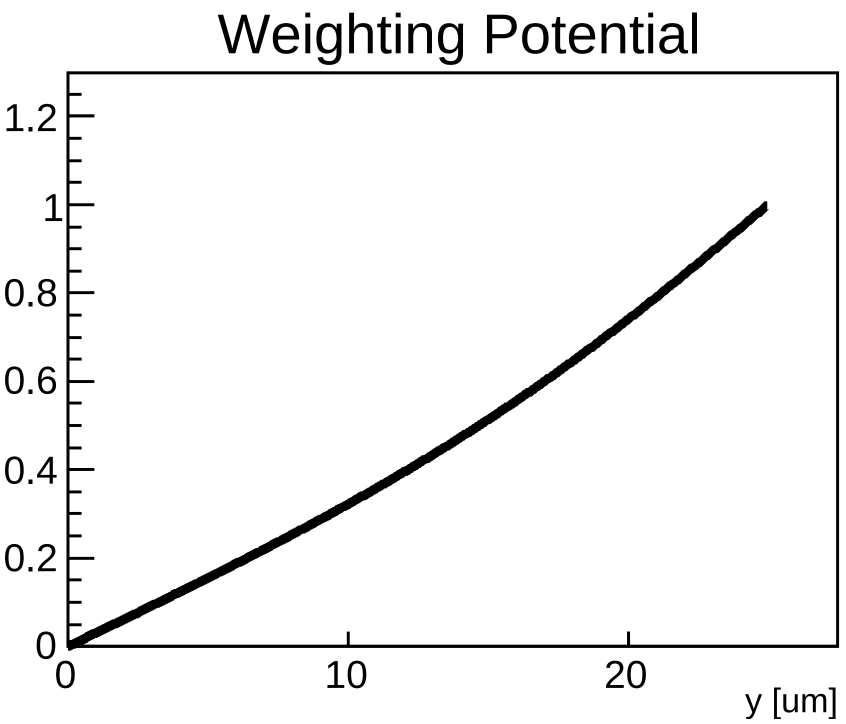

Figure 4.11: Weighting potential, Width=45μ m, stripes=10

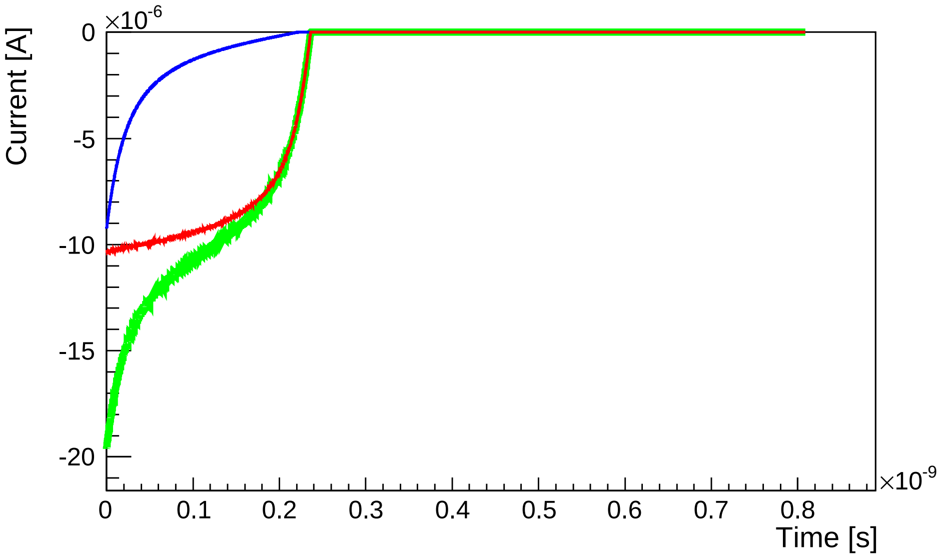

Figure 4.12: Currents, Width=45μ m, stripes=10

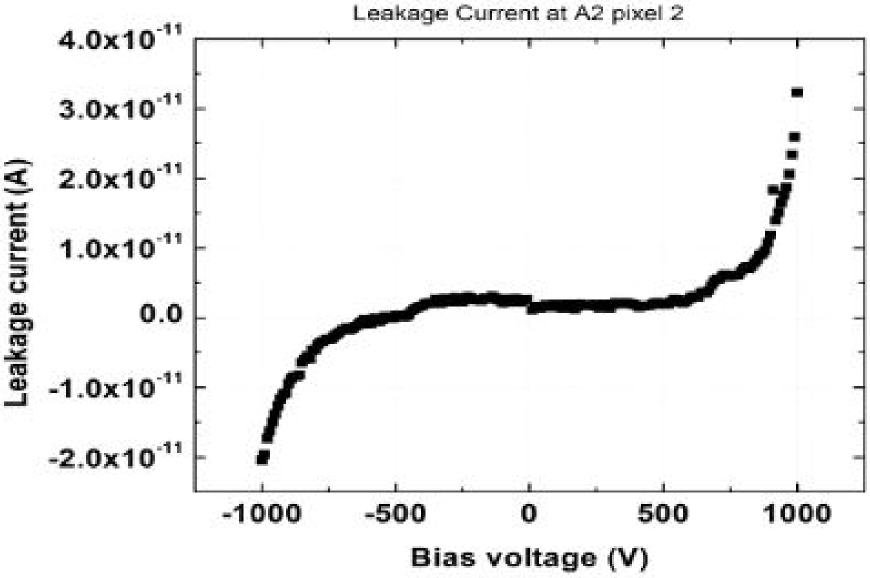

Figure 4.13: Leakage Current

Chapter 5

Summary

The aim of the thesis work was a better understanding of the diamond detector basics, working and limitations. From all the work going around the world and results from the papers we can say that artificial diamond is by far the best detector material available at the moment. The hardness of diamond make it highly resisitive against radiation damage. Other properties such as strong covalent bond and large band gap make diamond very suitable for high temperature and low senstivity experimentation.
The major limitation of current generation diamond detectors is the leakage current. There are a few methods to minimize the leakage current such as use of 3D diamond detectors. There are few labs across the world that are currently working on producing 3D diamond detectors.

There is still scope for improvement in the Weightfield 2 simulator, the main problem faced by diamond detectors is the huge surface leakage current. The simulator should take in account for leakage current so that we can study factors responsible for leakage current and understand ways to minimized it.

Bibliography

[1] . Antchev et al., First measurement of the total proton-proton cross section at the LHC energy of p s = 7 TeV, Europhys. Lett. 96 (2011) 21002

[2] OTEM collaboration, G. Antchev et al., Luminosity-independent measurements of total, elastic and inelastic cross-sections at p s = 7 TeV,

[3] OTEM collaboration, G. Antchev et al., Measurement of proton-proton elastic scattering and total cross-section at p s = 7 TeV,

[4] OTEM collaboration, G. Antchev et al., Luminosity-Independent Measurement of the Proton-Proton Total Cross section at p s = 8 TeV,

[5] . Antchev, P. Aspell, I. Atanassov, V. Avati, Diamond detectors for the TOTEM timing upgrade , Journal of Instrumentation , 2017 JINST 12 P03007

[6] mit Kumar,ArvindSingh,ArvindKumar,AnitaTopkar , Fabrication and characterization of polycrystalline diamond detectors for fast neutron monitoring , Electronics Division, Bhabha Atomic Research Centre,Trombay, Mumbai400085,India , 5 March 2015

[7] ara Bruzzi,HartmutF.W.Sadrozinski,AbrahamSeiden,NuclearInstruments and MethodsA579(2007)754.

[8] ainer SWallny,NuclearInstrumentsandMethodsA582(2007)824.

[9] .Bergonzo,F.Foulon,A.Brambilla,D.Tromson,C.Jany,S.Haan,Diamondand RelatedMaterials9(2000)1003.

[10] Angelone,MPillon,MMarinelli,etal.,RadiationProtectionDosimetry110 (2004)233.

[11] asakatsu Tsubota a,n, JunichiH.Kaneko a, DaijirouMiyazaki a, TakehiroShimaoka a, High-temperature characteristics of charge collection efficiency using single

CVD diamond detectors , Nuclear Instruments and Methods in Physics Research A789(2015)50–56

[12] . Willander,M.Friesel,Q.Wahab,B.Straumal,JournalofMaterialsScience— Materials inElectronics17(2006)1.

[13] . Kagan,NuclearInstrumentsandMethodsA541(2005)221.

[14] .E. Chelnokov,A.L.Syrkin,MaterialsScienceandEngineeringB46(1997) 248.

[15] . Sumiya,N.Toda,S.Satoh,JournalofCrystalGrowth237–239 (2002)1281.

[16] . Ogasawara , T.W.Broiles , K.E.Coulter , M.A.Dayeh , M.I.Desai , S.A.Livi , D.J. McComas , B.C.Walther , Single crystal chemical vapor deposit diamond detector for energetic plasma measurement in space , Nuclear Instruments and Methods in Physics Research A777(2015)131–137

[17] .Pausch,W.Bohne,D.Hilscher,H.-G.Ortlepp,D.Polster,NuclearInstru- ments and-MethodsinPhysicsResearchA349(1994)281. http://dx.doi.org/ 10.1016/0168-9002(94)90634-3.

[18] .J.Tapper,ReportsonProgressinPhysics63(2000)1273. http://dx.doi.org/ 10.1088/0034-4885/63/8/203.

[19] .Mittermayer,A.Steininger,IEEETransactionsonInstrumentationand Measurement 48(1999)1103. http://dx.doi.org/10.1109/TNS.19.816121.

[20] . Kanxheri, L. Servoli, C. Zucchetti, A. C. Dipilato, M. Iacco, S. Lagomarsino , A. Morozzi, D. Passeri , S. Sciortino , Evaluation of 3D diamond detectors for application in medical radiation dosimetry , 5th ADAMAS Workshop at GSI December 15-16, 2016, Darmstadt, Germany

[21] erner Riegler, CERN , Fundamentals of Particle Detectors and Developments in Detector Technologies for Future Experiments , 4/28/2008

[22] . Angelone, D. Lattanzi, M. Pillon, M. Marinelli, E. Milani, A. Tucciarone, G. Verona-Rinati, S. Popovichev, R.M. Montereali, M.A. Vincenti, A.Murari and JET EFDA contributors , Development of Single Crystal Diamond Neutron Detectors and Test on

the JET Tokamak , JET-EFDA, Culham Science Centre, OX14 3DB, Abingdon, UK , EFDA–JET–PR(07)56

[23] J Tapper , Diamond detectors in particle physics , H H Wills Physics Laboratory, University of Bristol, Tyndall Avenue, Bristol BS8 1TL, UK , 6 January 2000

[24] ield J E (ed) 1992 The Properties of Natural and Synthetic Diamond (New York: Academic)

[25] avis G (ed) 1994 The Properties and Growth of Diamond (London: JEE)

[26] pear K E and Dismukes J P 1994 Synthetic Diamond-Emerging CVD Science and Technology (New York: Wiley)

[27] all G 1994 Semiconductor particle tracking detectors Rep. Prog. Phys. 57 481–531

[28] eddy R J and Nam T L 1993 Diamond radiation detectors Radiat. Phys. Chem. 41 767–73

[29] erner M and Locher R 1998 Growth and application of doped and undoped diamond films Rep. Prog. Phys. 61 1665–710

[30] amamoorthy Ravichandran, John Pichy Binukumar, Iqbal Al Amri, Cheriyathmanjiyil Antony Davis , Diamond detector in absorbed dose measurements in high-energy linear accelerator photon and electron beams , JOURNAL OF APPLIED CLINICAL MEDICAL PHYSICS, VOLUME 17, NUMBER 2, 2016

[31] rlabrand A. Dosimetric characteristics of CVD single crystal diamond detectors in radiotherapy beams [MSc Thesis]. Stockholm, Sweden: Stockholm University; 2007.

[32] aub WU and Wong T. The volume effect of detectors in the dosimetry of small fields used in IMRT. Med Phys. 2003;30(3):341–47.

[33] riedl M. Diamond detectors for ionizing radiation [Diploma Thesis]. Vienna: University of Technology; 1999.

[34] elix Bachmair , CVD Diamond Sensors In Detectors For High Energy Physics , ETH No. 23725 , 2016, Institute for Particle Physics, Department of Physics, ETH Zürich

[35] ollaboration ATLAS. Letter of Intent for the Phase-II Upgrade of the ATLAS Experiment. Technical Report CERN-LHCC-2012-022. LHCC-I-023, CERN, Geneva, Dec 2012. URL https://cds.cern.ch/record/1502664.

[36] Butler, D Contardo, M Klute, J Mans, and L Silvestris. Technical Proposal for the Phase-II Upgrade of the CMS Detector. Technical Report CERN-LHCC-2015-010. LHCCP- 008, CERN, Geneva. Geneva, Jun 2015.

[37] shish Kumar Suny. Near future upgrades of the CMS pixel detector. talk at PIXEL 2014, Sept 2014. URL https://indico.cern.ch/event/302139/contributions/691616/attachments/570968/786464/Pixel2014$_v3.pdf$.

[38] ock Kiam Gan. Diamond particle detectors systems in high energy physics. PoS, TIPP2014:103, 2015. 11, 12, 259